Improving Consistency of Viewpoint Selection for Molecules

Vincent Larroque[1*], Maxime Maria[1*], Stéphane Mérillou[1] and Matthieu Montes[2,3,4]

[1]Laboratoire XLIM, UMR CNRS 7252, Université de Limoges, Limoges, France.
[2]Laboratoire Génomique, Bioinformatique et Chimie Moléculaire, EA7528, Conservatoire National des Arts et Métiers, Hésam Université, Paris, France.
[3]Institut Universitaire de France, Paris, France.
[4]Laboratory of Computational, Quantitative and Synthetic Biology, UMR 7238 CNRS, Sorbonne Université, Paris, France.

*Corresponding author(s). E-mail(s): vincent.larroque@unilim.fr; maxime.maria@unilim.fr;
Contributing authors: stephane.merillou@unilim.fr; matthieu.montes@sorbonne-universite.fr;

Abstract

Molecular visualization is widely used in structural molecular biology and drug discovery to study the structure of molecules and help their understanding. However, identifying meaningful viewpoints is challenging because of their abstract and convoluted nature of molecular scenes. Consequently, viewpoint selection methods have been developed to highlight important features of molecules. These methods base the selection process on metrics, which are functions that assign a score based on what can be observed in an image of a molecule. In this paper, we study 20 state-of-the-art metrics across four common molecular representations: Ball & Stick, van der Waals, Solvent Excluded Surface, and Cartoon. We evaluate the consistency of these metrics in identifying two crucial geometrical configurations for molecular studies: alignment and tunnel. We show that these metrics do not provide consistent results in finding these features. Therefore, we propose to optimize linear metric combination models, which significantly improves the overall detection performance.

Keywords: Molecular visualization, Viewpoint selection, Metric combination, Optimization.

1 Introduction

Molecular visualization has become increasingly important in many fields, such as drug design. Visualization software enables users to explore large molecular systems, understand their complex structures and share their findings with others, including peers and the general public [1].

There are different ways to represent molecules, depending on the information that needs to be highlighted. Some important representations are: Ball & Stick shows atoms as spheres and their chemical bonds as cylinders (figure 1a); van der Waals displays atoms as spheres of size proportional to their van Der Waals radius (figure 1b); the Solvent Excluded Surface shows the boundary surface of a molecule with respect to a solvent (figure 1c); Cartoon exposes the secondary structure of the molecule as ribbons,

arrows, and coils (figure 1d). For more information about molecular visualization, we refer the reader to Kozlíková *et al.* state of the art [2].

Visualizing molecules is a challenging task, even for experts: molecular systems are visually abstract and complex objects, whatever their representation. Previous surveys [3, 4] have shown that automatic viewpoint selection can help to find meaningful views of objects for movies, video games, or computer-aided design.

Viewpoint selection tasks are mainly done using metrics. A metric is a function that takes an image generated from a viewpoint as input and returns a score indicating its relevance according to specific criteria.

A previous study on viewpoint selection methods for 20 state-of-the-art metrics from the general field adapted for molecular visualization has shown promising results [5]. This work aims to find alignments (figure 2) and tunnels (figure 3) in molecules represented by either Ball & Stick or van der Waals models. They have concluded that no metric can reliably find both configurations simultaneously.

In this work, we propose to extend this study to two other common molecular representations: the Solvent Excluded Surface and Cartoon. Additionally, we present a method to optimize linear combination models of metrics to improve their consistency in finding both configurations.

The paper is organized as follows. We first present related works regarding viewpoint selection methods and their applications (section 2). Then, section 3 provides the study of the metrics. Section 4 presents models for combining metrics to improve their detection performance. Finally, section 5 concludes this paper and provides insights into future work.

2 Related Work

Viewpoint selection has been a subject of research for decades. Some studies have shown that users have view preferences when visualizing objects [6, 7]. Viewpoints are considered relevant when they provide important information about the object, improving its understanding.

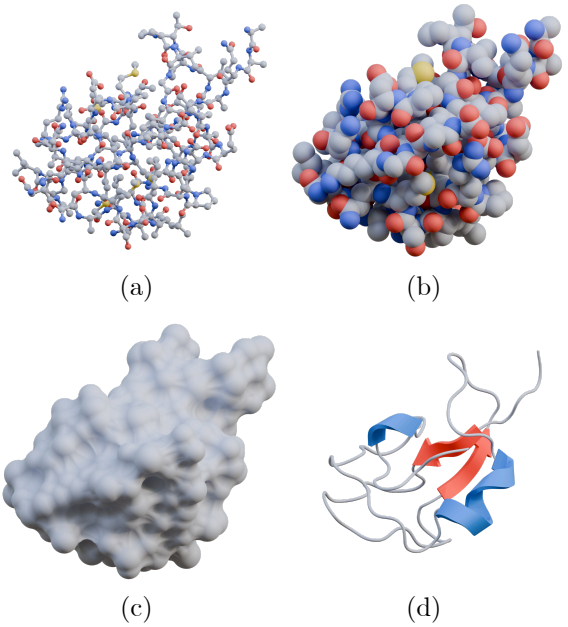

(a) (b) (c) (d)

Fig. 1: Different molecular representations of the same molecule: (a) Ball & Stick; (b) van der Waals; (c) Solvent Excluded Surface; (d) Cartoon.

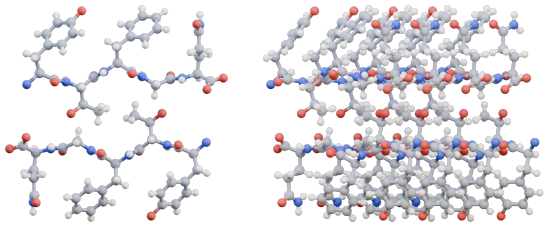

(a) (b)

Fig. 2: (a) An alignment, where the foreground hides the background; (b) a global viewpoint of the same molecule.

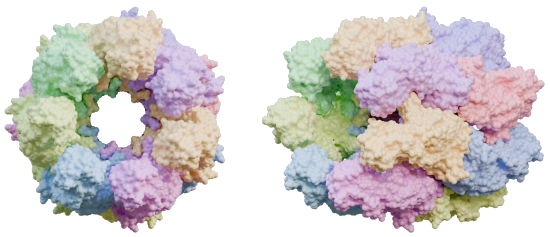

(a) (b)

Fig. 3: (a) A tunnel, with a hole going through the molecule; (b) a global viewpoint of the same molecule.

2.1 Viewpoint selection for general objects

Viewpoint selection was first applied to assets used in movie production, video games, and computer-aided design. This paper refers to these assets as "general" objects.

Kamada and Kawai [8] have presented one of the first works on viewpoint selection. They have proposed a method to find views that minimize the number of degenerated faces shown (*i.e.* aligned faces visible using an orthographic camera). Plemenos and Benayada [9] have introduced several metrics based on the projected surface information to display most of an object. Later, Vázquez *et al.* [10] have designed a new metric called *Viewpoint entropy* based on Shannon entropy [11] to find informative viewpoints. Since then, information theory has been widely used to create new metrics, as presented in the surveys of Secord *et al.* [3] and Bonaventura *et al.* [4].

Several works have also presented viewpoint selection for other kinds of visualization. For instance, Stoev and Straßer [12] have used it for terrain models, Viola *et al.* [13] for volumetric data and Marsaglia *et al.* [14] for large-scale scientific datasets.

2.2 Viewpoint selection for molecules

In the case of molecular visualization, interesting viewpoints generally highlight specific geometrical configurations. Viewpoints showing most of a molecule can also be relevant, as they give global information about its structure.

Vázquez *et al.* [15] have introduced *Viewpoint entropy* to find alignments (figure 2, left) and global viewpoints (figure 2, right) using the Ball & Stick representation and an orthographic camera. Doulamis *et al.* [16] have extended Vázquez work by adding semantic information to the search process. They have also designed a non-linear classifier that is continuously trained from expert selection within a set of predicted good viewpoints. Heinrich *et al.* [17] have adapted *Viewpoint entropy* for the Cartoon representation using its residue features. Additionally, they have conducted a study on view preferences for molecules and concluded that tunnels (figure 3) are also an interesting feature to identify. Larroque *et al.* [5] have studied the performance of metrics designed for general objects applied to molecular visualization. Their study concludes that no single metric can simultaneously identify alignments and tunnels.

In this paper, we propose to continue this last study by extending the dataset and considering new molecular representations (section 3).

2.3 Metric combinations

Hartwig *et al.* [18] have conducted a user study revealing that no single metric tends to satisfy their preferences.

Polonsky *et al.* [19] have suggested that combining metrics could improve viewpoint selection performance. Secord *et al.* [3] conducted a user study to establish a ground truth baseline to optimize metric combinations. They have also concluded that combining up to five metrics using a simple linear model improves the prediction performance. Marsaglia *et al.* [14] have shown that specialized metrics can be combined with general metrics to achieve better performance when searching for viewpoints around scientific data.

The purpose of our work is to determine if metric combination models can provide interesting results for molecular visualization, as they have not yet been applied to this field (section 4).

3 Metrics benchmark

In this section, we extend the work of Larroque *et al.* [5], which evaluated the ability of single metrics to identify alignments (figure 2) and tunnels (figure 3) in 63 molecules using the Ball & Stick and van der Waals representation. Alignments can help visualize how the molecule is organized in space [15] while tunnels may correspond to functional pathways or cavities within the protein structure [17]. We analyze the same 20 metrics, divided into five categories (table 1), which have been shown to be effective in viewpoint selection for general or scientific data [3, 4, 14]. Specifically, we extend this study by:

- considering two additional molecular representations: the Solvent Excluded Surface and Cartoon;
- using an extended dataset of 105 molecules from the Protein Data Bank [20] with 47 for the alignment and 58 for the tunnel (appendix A1);

- proposing to annotate geometrical configurations on each molecule beforehand to simplify metrics performance computation.

By definition, some metrics need to consider individually identified elements (*e.g.* spheres or cylinders). Therefore, we need to determine what is an element in the two added representations. For the Solvent Excluded Surface, we propose to use its surface patches. For Cartoon, we use its residue features, as suggested in [17]. Note that these two representations are computed with ChimeraX [21].

In the following sections, we present our benchmark process and the results of our study. A nomenclature is provided in table 2.

Category	Metric name
Surface	Number of visible elements [9]
	Projected area [9]
	Plemenos and Benayada [9]
	Visibility ratio [9]
	Viewpoint entropy [10]
	Kullback-Leibler distance [22]
	Viewpoint mutual information [23]
	Information I_2 [24]
	Information I_3 [24]
Silhouette	Silhouette length [19]
	Silhouette entropy [19]
	Silhouette curvature [25]
	Silhouette curvature extrema [3]
Depth	Stoev and Straßer [12]
	Maximum depth [3]
	Depth distribution [3]
	Depth entropy [14]
Stability	Instability [23]
	Depth-based visual stability [26]
High-level	Largest cone of view [5]

Table 1: The 20 studied metrics grouped into five categories.

3.1 Setup

We use the same setup as described in [5]. Candidate viewpoints around the molecule are selected using an enclosing icosahedron of 642 vertices, as a tradeoff between computation time and sampling quality. The icosahedron is positioned to ensure at least one viewpoint from which the geometrical configuration (alignment or tunnel) can be identified. An orthographic camera is placed on each vertex to capture an image of the scene of 1280 × 720 pixels. The camera parameters are

Notation	Description
v, V	A viewpoint and a set of viewpoints
M	Set of molecules (appendix A)
R	Set of molecular representations
σ_v	Input configuration, $\sigma \sim M \times R$ at viewpoint v
q_i	A metric i
$\mathrm{GT}(\sigma_v)$	Ground truth value for a configuration
$\mathcal{C}$	Consistency value
$Q(\sigma_v)$	A linear metric combination model
w_i	Weight of metric i
$\mathrm{P}(\sigma_V)$	Prediction tensor for a configuration and each viewpoint in V
$\mathcal{L}$	Cost function

Table 2: Nomenclature.

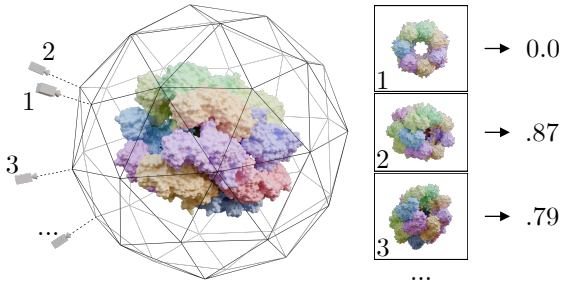

Fig. 4: Benchmarking process. Cameras are placed on the enclosing icosahedron vertices from which metrics are evaluated.

adjusted to fit the entire molecule. Finally, viewpoint images are then used by all the metrics to compute their corresponding scores. The benchmark process is illustrated in figure 4. Depending on the metric definition, the best viewpoints of a molecule can either be of highest or lowest score.

To enable comparison between the different metrics, we introduce a ground truth value at each vertex of the enclosing icosahedron. These values correspond to the visibility of each of the searched configurations. The maximum value of 1 is manually assigned to vertices where the hole going through the molecule is the most visible (figure 3, left). Since tunnels can have different shapes and sizes, we introduce a tolerance radius. On the neighboring vertices, we apply a quadratic decay function to the values, until the tunnel is no longer visible when moving the camera around the molecule (figure 5). In contrast, for the alignment, only the viewpoints where the foreground of the molecule completely hides the background

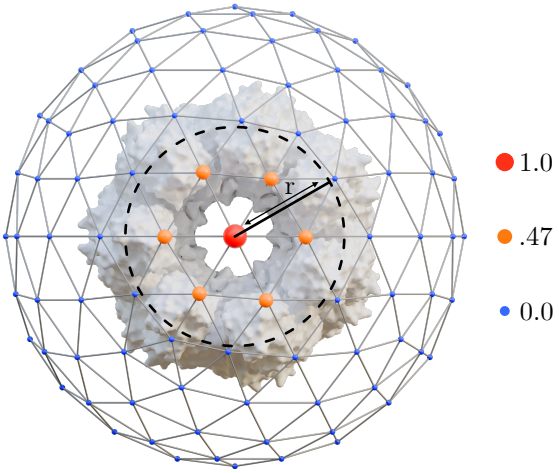

Fig. 5: Example performance value attribution for a molecule. The red sphere corresponds to the center of the tolerance radius r with quadratic decay for subsequent points.

(figure 2, left) are assigned a value of 1 and all other vertices 0.

In this work, we define M as the set of molecules, R as the set of representations, and V as the set of viewpoints. For a given sampled configuration $\sigma_v \sim M \times R$ at a viewpoint $v \in V$, the ground truth value is defined as $\mathrm{GT}(\sigma_v)$.

3.2 Performance measure

Two measures are used to indicate the metrics performance:

- Accuracy: the ability of a metric to identify a given geometrical configuration at **either** its highest or lowest scoring viewpoint for individual molecules.
- Consistency: the ability of a metric to reliably identify a given geometrical configuration **only** on its highest or lowest scoring viewpoint across all molecules.

In the context of this study, since a high consistency ensures that a viewpoint with a certain configuration can be reliably found, we focus on this performance measure.

We define $q_i(\sigma_v)$ as the function of a metric q_i taking a configuration σ_v to compute a score determining the image quality from a viewpoint v.

For a metric q_i, computing the consistency $\mathcal{C}_{i_{\max}}$ of its highest scoring viewpoint $v_{\max}$ involves averaging its ground truth values for each configuration:

$$\mathcal{C}_{i_{\max}} = \frac{1}{n} \sum_{j=1}^{n} \mathrm{GT}(\sigma_{v_{\max}}) \tag{1}$$

where n corresponds to the number of samples in $\sigma_{v_{\max}}$. Similarly, we can define the consistency of the minimum scoring viewpoints $v_{\min}$ as $C_{i_{\min}}$. The final consistency for a metric q_i is then defined as

$$\mathcal{C}_i = \max(\mathcal{C}_{i_{\max}}, \mathcal{C}_{i_{\min}}) \tag{2}$$

Using this equation, we can benchmark the performance of each studied metric.

3.3 Results

This section presents and analyses the results of our benchmark. Figure 6 sums up the consistency of each metric listed in table 1 for the alignment and for the tunnel. The plots correspond to an average over the four representations, where smaller error bars indicate more consistent results across them. Detailed results for individual representations are provided in appendix C.

Alignment

Maximum depth is the metric with the best consistency ($\mathcal{C} = 0.995$) because an aligned viewpoint has the lowest maximum depth compared to the others.

Metrics relying on surface information globally perform well ($\mathcal{C} > 0.9$), except for *Projected area*, *Stoev and Straßer* and *Information* I_3. The first two have more variance because van der Waals and Solvent Excluded Surface representations can create larger visible areas depending on the molecule shape, in contrast with Ball & Stick or Cartoon (figure 7). *Information* I_3 tries to capture specific information about elements visible from most viewpoints around the molecule. This makes it perform badly on smaller molecules, which constitute most of our dataset.

We can notice that since the Solvent Excluded Surface and Cartoon representations are meshes, some discretization issues may occur, slightly impacting the variance of some metrics such as *Viewpoint entropy* or *Information* I_2.

Most other metrics rely too much on factors that are not useful for finding alignments, such as

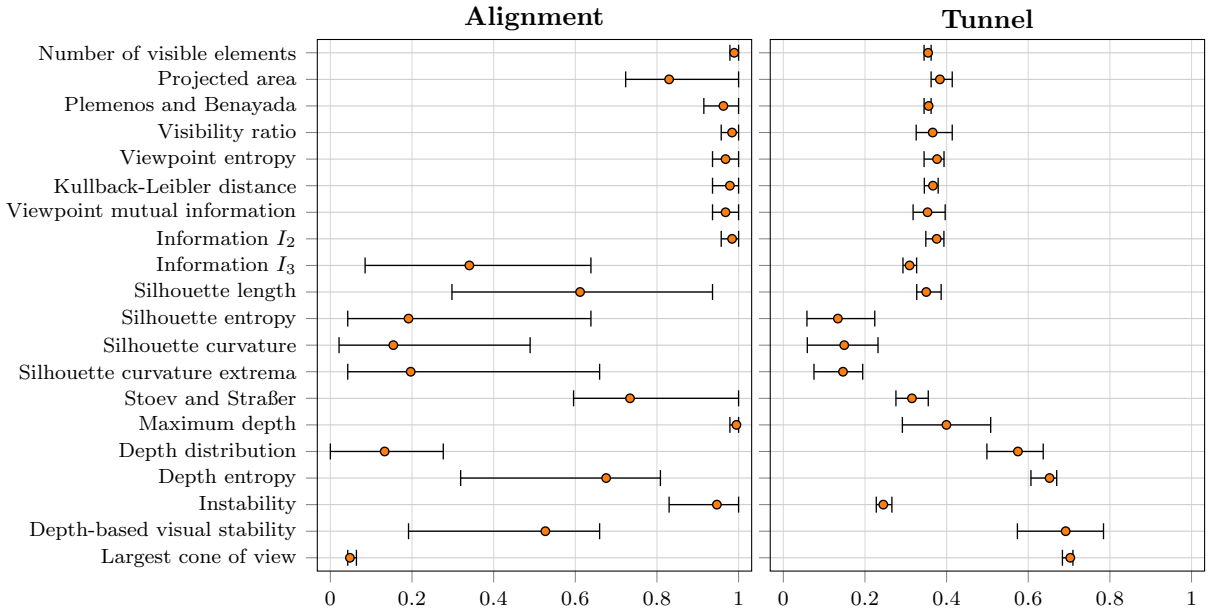

Fig. 6: Mean consistency for each metric over all representations. On the left, the results for the alignment and on the right, the results for the tunnel. The error bars represent the minimum and maximum consistency.

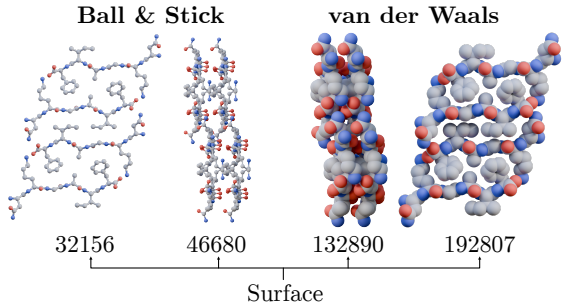

Fig. 7: The surface difference (in pixels) between a front view and a side view for Ball & Stick and van der Waals.

analyzing the depth range or the turning angles between consecutive pixels in the silhouette category. These metrics, by themselves, should be avoided for finding this configuration.

To conclude, most surface metrics can be used to find the alignment along with *Maximum depth* as they provide near-perfect consistency.

Tunnel

Only four metrics have a consistency above 0.5. *Largest cone of view* has the best consistency ($\mathcal{C} = 0.7$) and a low variance. However, by definition, it fails when the tunnel is not centered and does not provide good global viewpoints. *Depth-based visual stability* gives good results ($\mathcal{C} = 0.69$) but has a high variance and is the most computationally expensive as can be seen in table B2. Finally, *Depth distribution* and *Depth entropy* have lower consistency but can also provide good global viewpoints.

All other metrics have poor consistency ($\mathcal{C} < 0.5$) and should be avoided. This is due to the complexity of identifying tunnels, as they have no special properties regarding most metrics definitions. Since there is no correlation between the visible surface and the presence of a tunnel, metrics relying on surface or silhouette information can fail to find it. Finally, metrics relying on maximum depth do not perform well, as a wide range of depth values can be seen from most viewpoints.

To sum up, *Depth entropy* should be used as it is more versatile with good consistency. However if only finding tunnels is needed, *Largest cone of view* should be preferred.

These results confirm that, as shown in [5], most single metrics have limitations or edge cases

that can degrade their performance. Moreover, no metric has convincing results in finding both alignment and tunnels. This motivates the investigation of metric combinations to improve the automatic viewpoint selection process.

4 Metric combinations

This section presents an optimization process for finding metric combinations for the detection of both alignment and tunnels in molecules. The goal is to search for models that provide the highest possible consistency.

Polonsky *et al.* [19] hypothesized that it could be possible to combine several metrics to benefit from their individual advantages. Secord *et al.* [3] confirmed this idea in their study on general objects, which used linear combination models to improve viewpoint selection performance. Similarly, Marsaglia *et al.* [14] found comparable results in their research on viewpoint selection methods for large-scale datasets. However, it is not yet clear whether this approach can be applied to molecular visualization.

In this work, we propose to create a linear combination model of metrics that can find both geometrical configurations in molecules, regardless of their representation. To optimize this model, we need to define a cost function.

4.1 Cost function

Our linear combination model is based on a weighted sum of metrics defined as

$$Q(\sigma_v) = \sum_{i=1}^{n} w_i \, q_i(\sigma_v) \tag{3}$$

where n is the number of metrics in the model and w_i is the weight applied to a metric q_i. Each individual metric score is normalized to ensure coherent weight values during the optimization process. The goal is to find an optimal combination by adjusting the weights w_i according to the error between the predicted best viewpoints and the ground truth values.

To select the best predicted viewpoint, we apply softmax on $Q(\sigma_v)$ (equation 3) as an activation function for each $v \in V$. For a given configuration σ_V our prediction tensor $\mathrm{P}(\sigma_V)$ is then defined as

$$\mathrm{P}(\sigma_V) = \frac{e^{Q(\sigma_v)}}{\sum\limits_{k \in V} e^{Q(\sigma_k)}}, \quad \forall v \in V. \tag{4}$$

Finally, we define the cost function $\mathcal{L}$ as the mean squared error between the prediction $\mathrm{P}(\sigma_V)$ (equation 4) and the ground truth $\mathrm{GT}(\sigma_V)$:

$$\mathcal{L} = \frac{||\mathrm{GT}(\sigma_V) - \mathrm{P}(\sigma_V)||^2}{n} \tag{5}$$

where n is the number of configurations in $\sigma_V \sim M \times R$. This cost function is fast to compute as it only consists of tensor operations on precomputed data.

4.2 Optimization method

We consider the search for the best metric combination as a hyperparameter optimization process. We then need to test all the possible combinations of metrics to find the best one. In our case, it results in $\sum_{k=2}^{20} \binom{20}{k} = 1\,048\,555$ possible tests. Secord *et al.* [3] have stated that using more than 5 metrics does not improve the performance of linear models. This reduces the number of combinations to $\sum_{k=2}^{5} \binom{20}{k} = 21\,679$.

To obtain reliable results, we use a Nested Cross-Validation (Nested CV) method as it provides unbiased performance estimates for small datasets such as ours [27].

Nested CV splits the training process into two nested layers, each using a K-fold approach. In the outer layer, the molecular dataset is split into K folds where each fold is used as a test set once, while the others are used for training. In the inner layer, for each training set, the dataset is split again to find the best hyperparameters. We use $K = 5$ folds for the nested layers as it has lower computation times while still providing reliable results (figure 8).

To optimize the combination model in the inner layers of the Nested CV we propose to use RPROP [28]. RPROP is a parameter-free optimizer that uses an adaptive step size, which provides fast convergence rates. The optimizer aims to minimize the distance between the predicted best viewpoint $P(\sigma_v)$ and the ground-truth best viewpoint $\mathrm{GT}(\sigma_v)$. This distance is defined by the cost function $\mathcal{L}$ (equation 5) and is reduced

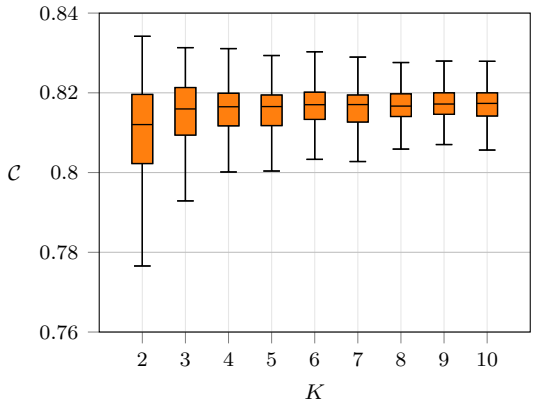

Fig. 8: Consistency of a linear combination model of 5 metrics across 500 trials for different K-Fold K values.

by adjusting the weights of the combination model (equation 3).

The optimized weights provided by each inner fold are averaged and transmitted to their corresponding outer layer. Then, for each outer test set, the consistency of each individual combination is computed using these weights. The final optimized metric combination is given by the average of the outer folds results.

4.3 Results

We use our optimization process to create three different viewpoint selection models: two specialized for finding alignments or tunnels and a general one to find both. Tables 3, 4 and 5 present the weights for the best single metric (1-comb) to the best combinations of up to five metrics (5-comb) and their corresponding consistency. For single metrics, a weight of -1 means that the minimum score viewpoint shows the geometrical configuration. These tables only present the best consistency found for each model, full results are available in the supplementary files.

Alignment model

Results for this model are shown in table 3. The individual metric *Maximum depth* provides near-perfect results with consistency of 0.995. In this case, a 2-combination is sufficient to have 100% consistency for the current dataset. Table 3 presents one of many possible combinations to get such results, as thousands can achieve perfect consistency. This performance is unsurprising, as the alignment is simple to detect for most single metrics when an orthographic camera is used (section 3.3).

Tunnel model

Table 4 shows the results of the tunnel model. The single metric *Largest cone of view* is the best to detect tunnels but has a consistency of only 0.703 (section 3.3). We can notice that its weakness can be offset by combining it with other metrics relying on surface or depth analysis. Starting from three metrics, the consistency exceeds 0.8. Combining more metrics only provides small advantages, given the increase in computation time.

General model

The consistency results for identifying both tunnels and alignments can be found in table 5. Using a single metric (*Maximum depth*) gives a consistency of 0.666. We can notice that only two metrics provide a significant increase in terms of detection performance. Combining four metrics allows to exceed 0.9 consistency, when combining five only offers small additional benefits.

The best combinations always include metrics based on surface or depth information along with *Largest cone of view*. Indeed, given that identifying alignment is relatively simple, the best metrics to combine in the general model are similar to those useful for finding tunnels.

We evaluate the statistical significance of the performance gain achieved by the optimized model. Paired t-tests compare the general model against each of the 20 single metrics across all molecules. For each molecule, predictions are averaged over the four considered representations before testing. The optimized model significantly outperforms most metrics ($p < 0.015$). No significant difference is observed for *Maximum depth* ($p = 0.79$), *Depth-based visual stability* ($p = 0.48$), and *Information* I_2 ($p = 0.17$). These tests support that the optimization provides a consistent, statistically supported improvement over most single metrics. The absence of significance for some metrics is expected: for instance, *Maximum depth*, already achieves near-ceiling performance for alignments and good results for tunnels, leaving limited room for improvement.

	1-comb	2-comb	3-comb	4-comb	5-comb
Maximum depth	-1				
Number of visible elements		-46.929	-73.674	-66.08	-56.023
Plemenos and Benayada		22.436	61.275	58.405	60.017
Projected area			-15.535	-13.538	-11.767
Viewpoint entropy				-4.332	
Visibility ratio					-8.411
Kullback-Leibler distance					7.694
Consistency	0.995	1.000	1.000	1.000	1.000

Table 3: Optimized weights and consistency for the **alignment** specialized model: results are given from one (1-comb) to five linear combinations (5-comb). Optimization has been performed on a dataset of 47 molecules (appendix A1).

	1-comb	2-comb	3-comb	4-comb	5-comb
Largest cone of view	1	12.709	11.373	11.553	11.566
Depth entropy		-8.389		-5.33	-4.52
Viewpoint entropy			-6.331		
Depth-based visual stability			8.039	3.412	4.467
Kullback-Leibler distance				7.496	
Plemenos and Benayada					-4.972
Instability					3.019
Consistency	0.703	0.790	0.836	0.858	0.869

Table 4: Optimized weights and consistency for the **tunnel** specialized model: results are given from one (1-comb) to five linear combinations (5-comb). Optimization has been performed on a dataset of 58 molecules (appendix A1)

This study shows that there are benefits in using specialized linear models for finding the two geometrical configurations compared to the general one. However, as shown in table 6, the gains are small. The general model is useful for the preliminary study of unknown molecules.

5 Conclusion

In this work, we have studied the performance of single metrics for finding two important geometrical configurations of molecules: the alignment and the tunnel. We showed that, for the alignment, several metrics are nearly perfectly consistent. However, identifying tunnels is more complex and no metric provides satisfying results.

To improve the global detection performance, we have proposed to combine metrics. We have studied three different linear models to find either alignment or tunnels, or both at the same time. While the specific models perform slightly better, they fail to generalize to any molecule which reduces their usability. We conclude that the global model should be used in most cases as it can highlight interesting configurations of unknown molecules.

In this work, we focused on a linear combination model. However, Secord *et al.* [3] suggested that non-linear approaches may yield better performance. Future studies could explore machine learning methods to design more complex and efficient combination models. In particular, AutoML techniques [29] could automate the search for optimal architectures and parameters, potentially improving viewpoint selection performance.

Computation time was out of scope for this work and has only been quickly discussed but could be an important parameter to consider in our optimization process. Appendix B provides indicative benchmarks of metric computational performance. Another way of improvement could be exploring other methods to select candidate viewpoints around molecules. Finally, providing new specialized metrics for other interesting molecular features could benefit their study

	1-comb	2-comb	3-comb	4-comb	5-comb
Maximum depth	-1			-4.806	
Projected area		-14.475			
Depth entropy		-22.775	-12.532		-6.034
Viewpoint mutual information			14.008		
Largest cone of view			8.854	9.18	6.505
Kullback-Leibler distance				11.181	
Depth-based visual stability				9.29	8.37
Plemenos and Benayada					-7.57
Instability					3.758
Consistency	0.666	0.848	0.893	0.906	0.912

Table 5: Optimized weights and consistency for the **general** model: results are given from one (1-comb) to five linear combinations (5-comb). Optimization has been performed on a dataset of 105 molecules (appendix A1).

Dataset	**Full**	**Alignment**		**Tunnel**	
Model	Gen.	Spec.	Gen.	Spec.	Gen.
1-comb	0.666	0.995	0.995	0.703	0.400
2-comb	0.848	1.000	0.995	0.790	0.729
3-comb	0.893	1.000	0.973	0.840	0.827
4-comb	0.906	1.000	0.984	0.855	0.842
5-comb	0.912	1.000	0.973	0.868	0.862

Table 6: Consistency comparisons of the general (Gen.) model performance against the specialized (Spec.) models. These results were computed on their respective full datasets (Alignment and Tunnel) using the best-found weights in table 3, 4 and 5.

for instance, by facilitating the identification and visualization of interaction zones or carbon chains.

Supplementary information. The code and full results for our metric combination process (detailed in section 4) are available in the accompanying supplementary material. The results files contain the weights for each metric combination, as well as the resulting accuracy and consistency which are obtained by running the optimization process from the source code.

Declarations

Conflict of interest. The authors declare that they have no conflict of interest.

Competing interests. The authors declare that they have no competing interests.

Funding information. Vincent Larroque is supported by institutional grants from the National Research Agency under the Investments for the future program with the reference ANR-18-EURE-0017 TACTIC and a fellowship from Qubit Pharmaceuticals. Matthieu Montes is supported by the European Research Council Executive Agency under grant numbers 640283 and 101069190.

Author contribution. All authors contributed to the study conception and design. Material preparation, data collection and analysis were performed by Vincent Larroque. The first draft of the manuscript was written by Vincent Larroque and all authors commented on previous versions of the manuscript. All authors read and approved the final manuscript.

Data availability. The dataset used in this work has been created using molecules from the Protein Data Bank [20].

Research involving human and /or animals. Not applicable.

Informed consent. Not applicable.

Appendix A Dataset

Table A1 gives the PDB IDs [20] of the molecules used for the detection of alignments and tunnels. The global dataset contains 105 molecules.

Appendix B Metric computation times

Table B2 presents indicative benchmark results for the computation times of the metrics listed in

Alignment dataset (47 elements)
5K2E, 7SXN, 4XFO, 6FGR, 6RHD, 4W71, 5I55, 2ONX, 2ONW, 6NB9, 4W5L, 6RHB, 3FVA, 6DIY, 4ZNN, 4ROP, 6GQ5, 7LUX, 6C4O, 6BZM, 3NHD, 3OVL, 6OIZ, 5VSG, 4RIL, 6C3S, 6BTK, 6FHC, 5E5Z, 1A3J, 5KOO, 3FPO, 6C3F, 5V5B, 7LTU, 8DDF, 3Q2X, 6FHD, 5K7N, 6BWZ, 8DDG, 4NIO, 4QXX, 5TXD, 3DG1, 3NVG, 6PQA

Tunnel dataset (58 elements)
5JJ1, 6UWT, 1GEH, 1LJ7, 1A2V, 5WJT, 2X2C, 7SQC, 6X6K, 2NN6, 6U42, 5TCR, 7Q4U, 2WCD, 1BGA, 6ZW7, 1EI7, 5CQF, 6X63, 6S6M, 1KP8, 1AON, 1AOS, 7T7C, 5WQ8, 6X62, 8PHU, 4P9Y, 1HKX, 1BHC, 1GRL, 6TMW, 7QXF, 1F1H, 1C9S, 1AVO, 5LKI, 6QZ9, 4V4K, 7AX3, 1B25, 6U5F, 1HI9, 1DW9, 7SN9, 2GTL, 7MUS, 1AA1, 7PKR, 1FOU, 1AW5, 5FKI, 7LER, 1A6R, 7SP4, 7AZD, 1CGM, 1AOO

Table A1: Molecules PDB IDs [20] for the detection of alignments (top) and tunnels (bottom).

table 1. The tests were conducted on a computer equipped with an AMD Ryzen 7 3700X CPU and 32 GB of RAM. All metrics were implemented in the same way for CPU execution with limited parallelism. These results should be considered as rough guidelines, since no specific optimization for computational efficiency was performed.

Time (ms)	**Metrics**
0.2 to 0.3	*Projected area*, *Visibility ratio*, *Stoev and Straßer*, *Maximum depth*
0.3 to 0.5	*Number of visible elements*, *Plemenos and Benayada*, *Silhouette length*, *Silhouette entropy*, *Silhouette curvature*, *Silhouette curvature extrema*
0.6 to 1.0	*Viewpoint entropy*, *Kullback–Leibler distance*, *Viewpoint mutual information*, *Information* I_2, *Depth distribution*, *Depth entropy*, *Largest cone of view*
4.1	*Information* I_3
6.6	*Instability*
900	*Depth-based visual stability*

Table B2: Computation time per viewpoint of different metrics on `1AON` (average over 642 viewpoints).

Appendix C Full benchmark results

Figure C1 and figure C2 present the accuracy and consistency results of each metric in table 1 and each representation separately for the detection of alignments and tunnels respectively.

References

[1] Olson, A.J.: Perspectives on structural molecular biology visualization: From past to present. J. Mol. Biol. **430**(21), 3997–4012 (2018) https://doi.org/10.1016/j.jmb.2018.07.009

[2] Kozlíková, B., Krone, M., Falk, M., Lindow, N., Baaden, M., Baum, D., Viola, I., Parulek, J., Hege, H.-C.: Visualization of biomolecular structures: State of the art revisited. Comput. Graph. Forum **36**(8), 178–204 (2017) https://doi.org/10.1111/cgf.13072

[3] Secord, A., Lu, J., Finkelstein, A., Singh, M., Nealen, A.: Perceptual models of viewpoint preference. ACM Transactions on Graphics **30**(5), 1–12 (2011) https://doi.org/10.1145/2019627.2019628

[4] Bonaventura, X., Feixas, M., Sbert, M., Chuang, L., Wallraven, C.: A survey of viewpoint selection methods for polygonal models. Entropy-switz. **20**(5), 370 (2018) https://doi.org/10.3390/e20050370

[5] Larroque, V., Maria, M., Mérillou, S., Montes, M.: Viewpoint selection for molecular visualization: Analysis and applications. In: Proceedings of the 19th International Joint Conference on Computer Vision, Imaging and Computer Graphics Theory and Applications, pp. 58–69 (2024). https://doi.org/10.5220/0012383300003660

[6] Blanz, V., Tarr, M.J., Bülthoff, H.H.: What object attributes determine canonical views? Perception **28**(5), 575–599 (1999) https://doi.org/10.1068/p2897

[7] Cutzu, F., Edelman, S.: Canonical views in object representation and recognition. Vision Research **34**(22), 3037–3056 (1994) https://doi.org/10.1016/0042-6989(94)90277-1

[8] Kamada, T., Kawai, S.: A simple method for computing general position in displaying three-dimensional objects. Computer

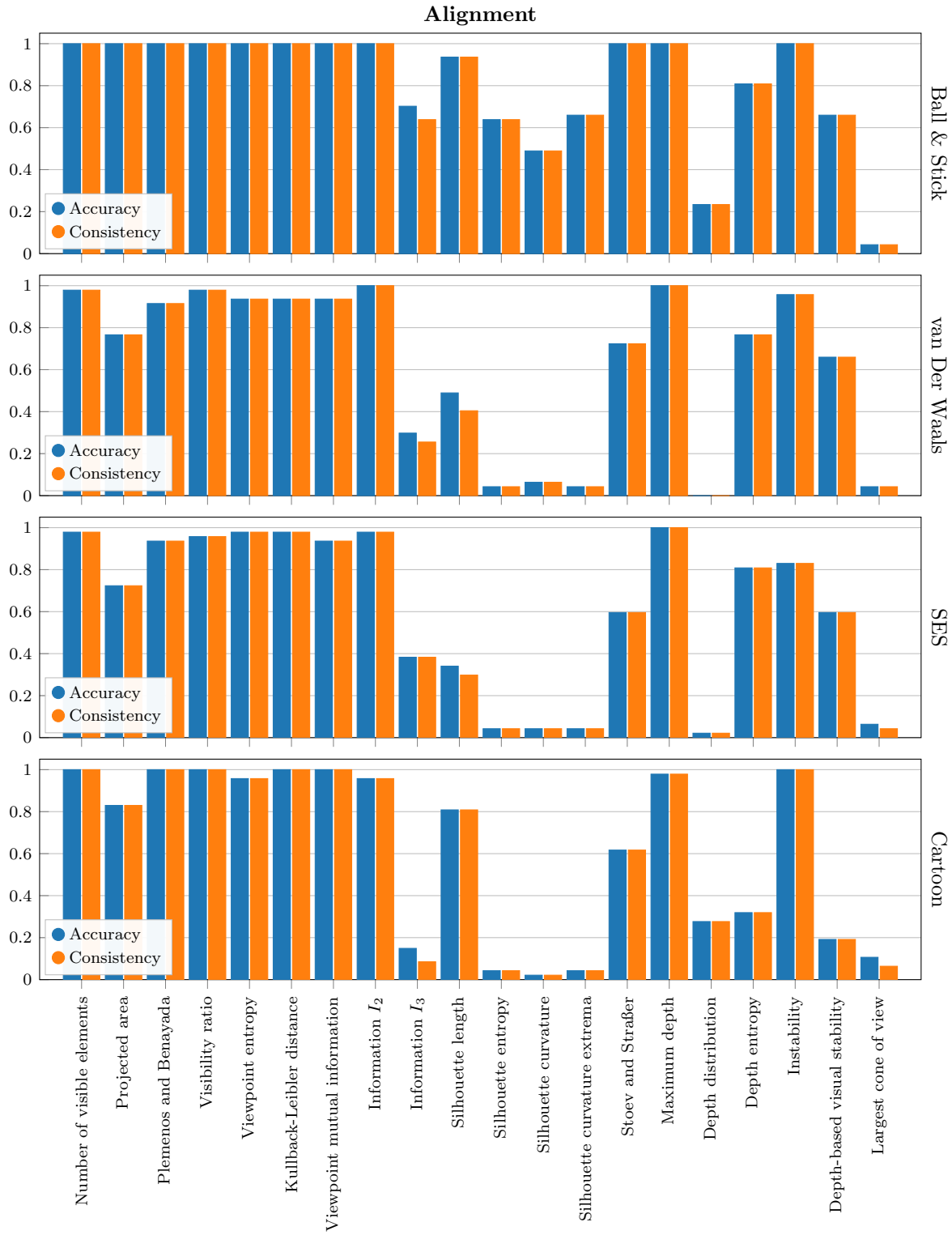

Fig. C1: Accuracy and consistency of the 20 evaluated metrics for each representation to detect alignments using the dataset in table A1.

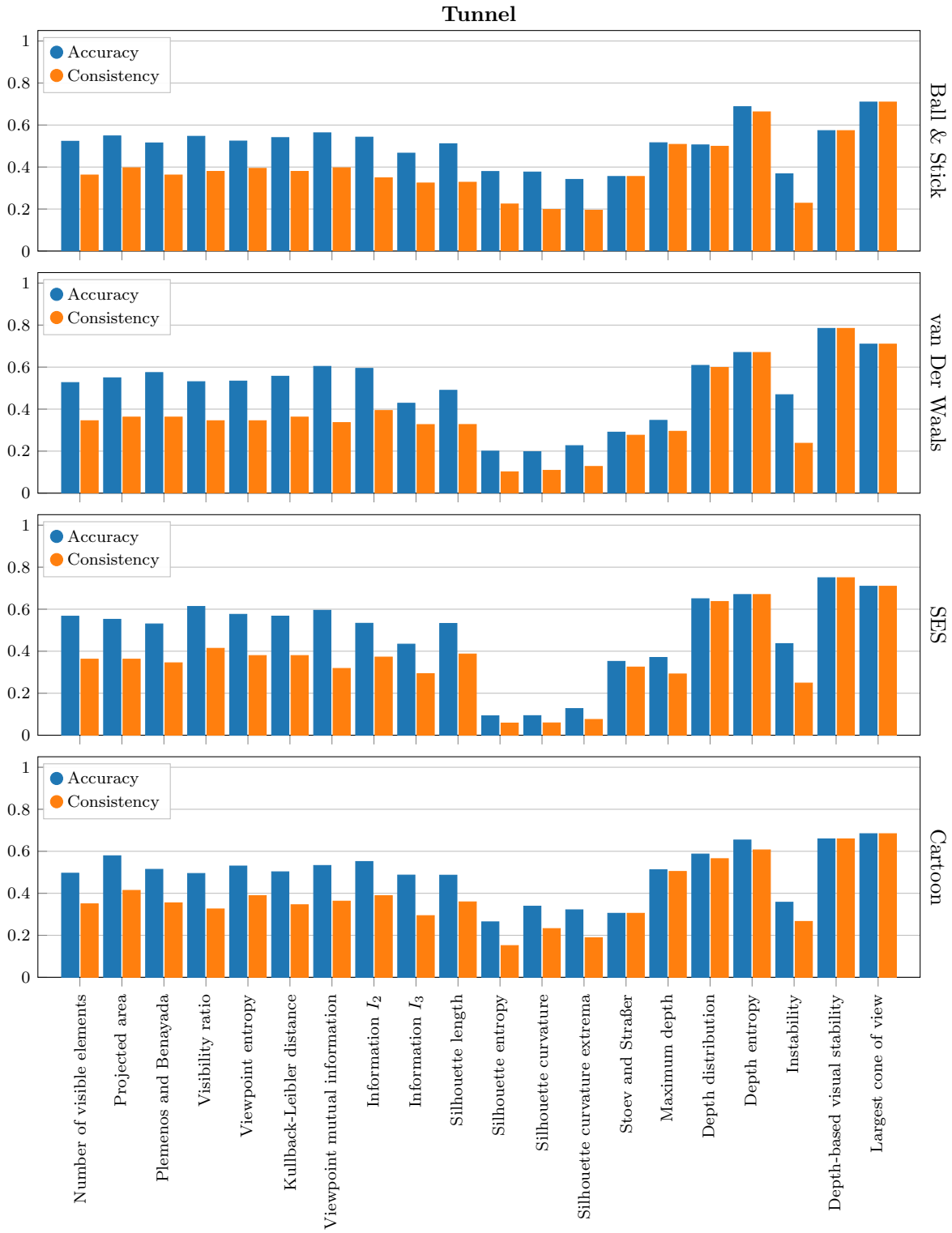

Fig. C2: Accuracy and consistency of the 20 evaluated metrics for each representation to detect tunnels using the dataset in table A1.

Vision, Graphics, and Image Processing **41**(1), 43–56 (1988) https://doi.org/10.1016/0734-189x(88)90116-8

[9] Plemenos, D., Benayada, M.: Intelligent display in scene modeling. new techniques to automatically compute good views. In: In Proceedings of the International Conference GraphiCon'96, St Petersbourg, Russia (1996)

[10] Vázquez, P.-P., Feixas, M., Sbert, M., Heidrich, W.: Viewpoint selection using viewpoint entropy. In: Proceedings of the Vision Modeling and Visualization Conference 2001. VMV '01, pp. 273–280 (2001)

[11] Shannon, C.E.: A mathematical theory of communication. Bell Syst. Tech. J. **27**(3), 379–423 (1948) https://doi.org/10.1002/j.1538-7305.1948.tb01338.x

[12] Stoev, S.L., Straßer, W.: A case study on automatic camera placement and motion for visualizing historical data. In: IEEE Visualization, 2002. VIS 2002., pp. 545–548 (2002). https://doi.org/10.1109/VISUAL.2002.1183826

[13] Viola, I., Feixas, M., Sbert, M., Groller, M.E.: Importance-driven focus of attention. IEEE Trans. Visual Comput. Graphics **12**(5), 933–940 (2006) https://doi.org/10.1109/tvcg.2006.152

[14] Marsaglia, N., Kawakami, Y., Schwartz, S.D., Fields, S., Childs, H.: An entropy-based approach for identifying user-preferred camera positions. In: 2021 IEEE 11th Symposium on Large Data Analysis and Visualization (LDAV), pp. 73–83 (2021). https://doi.org/10.1109/LDAV53230.2021.00015

[15] Vázquez, P.-P., Feixas, M., Sbert, M., Llobet, A.: Viewpoint entropy: a new tool for obtaining good views of molecules. In: Proceedings of the Symposium on Data Visualisation 2002. VISSYM '02, pp. 183–188. Eurographics Association, Goslar, DEU (2002). https://doi.org/10.2312/VisSym/VisSym02/183-188

[16] Doulamis, N., Chronis, E., Miaoulis, G., Plemenos, D.: In: Plemenos, D., Miaoulis, G. (eds.) Personalized View Selection of 3D Molecular Proteins, pp. 211–227. Springer, Berlin, Heidelberg (2010). https://doi.org/10.1007/978-3-642-15690-8_11

[17] Heinrich, J., Vuong, J., Hammang, C.J., Wu, A., Rittenbruch, M., Hogan, J., Brereton, M., O'Donoghue, S.I.: Evaluating viewpoint entropy for ribbon representation of protein structure. Comput. Graph. Forum **35**(3), 181–190 (2016) https://doi.org/10.1111/cgf.12894

[18] Hartwig, S., Schelling, M., Onzenoodt, C.v., Vázquez, P.-P., Hermosilla, P., Ropinski, T.: Learning human viewpoint preferences from sparsely annotated models. Comput. Graph. Forum **41**(6), 453–466 (2022) https://doi.org/10.1111/cgf.14613

[19] Polonsky, O., Patané, G., Biasotti, S., Gotsman, C., Spagnuolo, M.: What's in an image?: Towards the computation of the "best" view of an object. The Visual Computer **21**(8–10), 840–847 (2005) https://doi.org/10.1007/s00371-005-0326-y

[20] Berman, H.M.: The protein data bank. Nucleic Acids Research **28**(1), 235–242 (2000) https://doi.org/10.1093/nar/28.1.235

[21] Meng, E.C., Goddard, T.D., Pettersen, E.F., Couch, G.S., Pearson, Z.J., Morris, J.H., Ferrin, T.E.: Ucsf chimerax: Tools for structure building and analysis. Protein Science **32**(11), 4792 (2023) https://doi.org/10.1002/pro.4792

[22] Sbert, M., Plemenos, D., Feixas, M., González, F.: Viewpoint quality: Measures and applications. In: Neumann, L., Sbert, M., Gooch, B., Purgathofer, W. (eds.) Computational Aesthetics in Graphics, Visualization and Imaging (2005). https://doi.org/10.2312/COMPAESTH/COMPAESTH05/185-192

[23] Feixas, M., Sbert, M., González, F.: A unified information-theoretic framework for viewpoint selection and mesh saliency. ACM

Transactions on Applied Perception **6**(1), 1–23 (2009) https://doi.org/10.1145/1462055.1462056

[24] Bonaventura, X., Feixas, M., Sbert, M.: Viewpoint information. 21st International Conference on Computer Graphics and Vision, GraphiCon'2011 - Conference Proceedings (2011)

[25] Vieira, T., Bordignon, A., Peixoto, A., Tavares, G., Lopes, H., Velho, L., Lewiner, T.: Learning good views through intelligent galleries. Comput. Graph. Forum **28**(2), 717–726 (2009) https://doi.org/10.1111/j.1467-8659.2009.01412.x

[26] Vázquez, P.-P.: Automatic view selection through depth-based view stability analysis. The Visual Computer **25**(5–7), 441–449 (2009) https://doi.org/10.1007/s00371-009-0326-4

[27] Vabalas, A., Gowen, E., Poliakoff, E., Casson, A.J.: Machine learning algorithm validation with a limited sample size. PLOS ONE **14**(11), 0224365 (2019) https://doi.org/10.1371/journal.pone.0224365

[28] Riedmiller, M., Braun, H.: A direct adaptive method for faster backpropagation learning: the rprop algorithm. In: IEEE International Conference on Neural Networks, pp. 586–5911 (1993). https://doi.org/10.1109/ICNN.1993.298623

[29] Siriborvornratanakul, T.: Human behavior in image-based road health inspection systems despite the emerging automl. Journal of Big Data **9**(1) (2022) https://doi.org/10.1186/s40537-022-00646-8